

Electronic, magnetic, and optical properties of Mn-doped GaSb: a first-principles study

Chuang Wang,¹ Wenhui Wan,¹ Yanfeng Ge,¹ Yong-Hong Zhao,² Kaicheng Zhang,³ and Yong Liu^{1, a)}

¹⁾*State Key Laboratory of Metastable Materials Science and Technology
& Key Laboratory for Microstructural Material Physics of Hebei Province,
School of Science, Yanshan University, Qinhuangdao 066004,
China*

²⁾*College of Physics and Electronic Engineering, Center for Computational Sciences,
Sichuan Normal University, Chengdu, 610068, China*

³⁾*College of Mathematics and Physics, Bohai University, Jinzhou 121013,
China*

Half-metallic ferromagnets can produce fully spin-polarized conduction electrons and can be applied to fabricate spintronic devices. Thus, in this study, the electronic structure, magnetic properties, and optical properties of GaSb, which has exhibited half-metallicity, doped with Mn, a 3d transition metal, are calculated using the generalized gradient approximation and Heyd-Scuseria-Ernzerhof (HSE) functional. $\text{Ga}_{1-x}\text{Mn}_x\text{Sb}$ ($x = 0.25, 0.5, 0.75$) materials exhibit ferromagnetic half-metallic properties and a high Curie temperature, indicating that this series can be applied in spintronic devices. Meanwhile, they absorb strongly in the infrared band, suggesting that $\text{Ga}_{1-x}\text{Mn}_x\text{Sb}$ also has potential applications in infrared photoelectric devices.

^{a)}Electronic mail: yongliu@ysu.edu.cn, or ycliu@ysu.edu.cn

INTRODUCTION

Over the past few decades, spintronics has developed rapidly. Compared with traditional semiconductor devices, spintronic devices have the advantages of storage non-volatility, lower power consumption, higher integration, etc.^{1,2}. In 1983, through their study of alloys such as Heusler alloys NiMnSb and PtMnSb, Groot et al. first discovered a material with a special energy band structure in which one direction of the electron spin band exhibits metallicity, while the other direction of the electron spin band is semiconducting. They thus named the material a half-metallic ferromagnet (HMF)^{3,4}. This type of material can produce fully spin-polarized conduction electrons, a good source of spin-flow injection⁵⁻⁷. With their magnetic moment quantization and zero magnetic susceptibility, HMFs can be used to fabricate spintronic devices such as spin diodes, spin field effect transistors, spin valves, and spin filters⁸⁻¹¹. Thus, not only will HMFs play an important role in a new generation of high-performance microelectronic devices but they will also open up new avenues in the research of polarization transport theory and spintronics¹²⁻¹⁵.

Unlike conventional electronics, spintronics utilizes the charge and spin of electrons to carry information and, thus, has superior performance. During the development of spintronic materials, new magnetic materials with both magnetic and semiconductor properties have been discovered, which has aroused great interest in the study of spintronics. Binary semiconductors doped with magnetic transition metal elements have also played an important role in spintronics development. Related research has found that a small number of magnetic elements can be incorporated into semiconductors such as Group II-VI, Group IV, or Group III-V elements¹⁶⁻¹⁸. In such systems, the incorporated magnetic atoms replace the cations or anions in the semiconductor unit cell, or defects form in the system, both of which have led to the discovery of many new spintronic materials. Investigations have revealed that III-V compound semiconductor materials have broad applications in optoelectronic devices, optoelectronic integration, ultrahigh-speed microelectronic devices and ultrahigh-frequency microwave devices and circuits^{19,20}.

In recent years, many new half-metallic (HM) materials have been discovered by doping III-V binary semiconductors with transition metal elements²¹⁻²⁴. However, few studies exist in the literature on the electronic properties of the III-V semiconductor material GaSb doped with 3d transition metals. GaSb is a direct band gap semiconductor with a zinc-blende (ZB)

crystal structure, a band gap of about 0.72 eV, and a lattice constant of 0.61 nm²⁵, GaSb has the characteristics of high electron mobility, high frequency and low threshold, and a high photoelectric conversion rate²⁶⁻²⁸. Meanwhile, the lattice constant of this material approximately matches those of other various ternary and quaternary III-V compound semiconductor materials, which can greatly mitigate the problematic stress and defects caused by lattice mismatch. Thus, GaSb has become an important substrate material for preparing long-wave light-emitting diodes (LEDs), photodetectors, and fiber-optic communication devices²⁹⁻³¹. Nonetheless, to the best of our knowledge, GaSb doped with the transition metal Mn has never been systematically researched about³²⁻³⁵. In this paper, we report first-principles calculations of Ga_{1-x}Mn_xSb ($x = 0.25, 0.5, 0.75$) compounds, which are observed to be HMFs and, thus, could be useful in both spintronics and infrared photoelectrics.

The remaining part of the paper is organized as follows: in Section II, we present our calculations in detail; in Section III, we describe the results and discuss the electronic, magnetic, and optical properties of these ZB ternary Ga_{1-x}Mn_xSb compounds. Finally, in Section IV, we summarize our results.

METHODS

GaSb has the ZB crystal structure, and its space group is $F\bar{4}3m$ (No. 216)^{36,37}. Each Ga (Sb) atom is at the center of a tetrahedron of its four nearest-neighbor Sb (Ga) atoms, as shown in Fig.1. For the calculations, we replace either one, two, or three Ga atoms with Mn atoms in the GaSb unit cell, for a Mn doping ratio of 25%, 50%, and 75%, respectively. Thus, we obtain a series of ZB Ga_{1-x}Mn_xSb ($x = 0.25, 0.5, 0.75$) compounds. The main contents of this paper are the study of the electrical, magnetic, and optical properties of ZB Ga_{1-x}Mn_xSb ($x = 0.25, 0.5, 0.75$) by first principles.

All calculations were performed using the first-principles calculation package VASP (Vienna ab initio simulation package)^{38,39}. For the simulation, we chose the projected augmented wave (PAW)⁴⁰ to describe the interaction between electrons and nuclei. The correlation between electrons and electrons uses a generalized gradient (generalized gradient approximation, GGA)⁴¹ in the form of the Perdew-Burke-Ernzerhof functional (PBE-96)⁴². First, we optimize the Monkhorst-Pack special K-point selection for the plane wave truncation energy and the Brillouin zone integral for each structural system. E_{cut} is set to 400

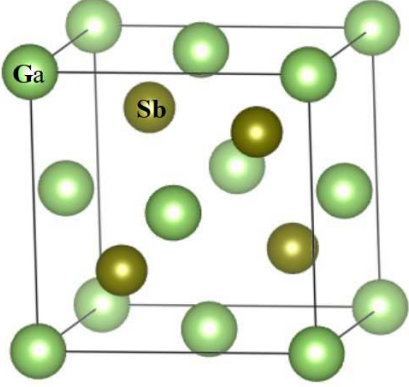


FIG. 1. Structure of zinc-blende GaSb.

eV, and the K point is $7 \times 7 \times 7$. In the crystal structure optimization and atomic relaxation process, the accuracies of the total energy convergence of the system and the force convergence on a single atom are 10^{-5} eV and 10^{-4} eV/atom, respectively.

We calculated the total energy of non-magnetic (NM), ferromagnetic (FM), and anti-ferromagnetic (AFM) states of ZB $\text{Ga}_{1-x}\text{Mn}_x\text{Sb}$ ($x = 0.25, 0.5, 0.75$) as a function of the lattice constant. Because the PBE functional calculation underestimates the crystal band gap, we added the Heyd-Scuseria-Ernzerhof (HSE) hybrid density functional^{43,44} to calculate the electron band. HSE is used to solve the numerical analysis of the Kohn-Sham⁴⁵ equation in the plane wave basis set and introduces the non-local exact exchange. Some of this equation is calculated by a precise exchange, thus, improving the electron self-interaction of the system. The total energy of the electronic system can be described well by HSE, and the calculated energy band is similar to that observed experimentally. Thus, the calculation results are reasonable.

RESULTS AND DISCUSSIONS

Magnetic properties. We calculated the electronic ground state properties of $\text{Ga}_{1-x}\text{Mn}_x\text{Sb}$ materials at different Mn concentrations. As Fig. 2(d) shows, the FM and AFM states are calculated mainly by making the spins of the even-numbered Mn parallel, anti-parallel, and cross-parallel. Figure 2(a), 2(b) and 2(c) show the energyCvolume curves corresponding to the three different magnetic states (NM, FM, AFM, respectively) of the $\text{Ga}_{1-x}\text{Mn}_x\text{Sb}$ at different Mn concentrations. The figure demonstrates that the FM state has the lowest

energy in all three states. Therefore, for equilibrium lattice constant, the FM state of ZB $\text{Ga}_{1-x}\text{Mn}_x\text{Sb}$ is the most stable.

TABLE I. $\text{Ga}_{1-x}\text{Mn}_x\text{Sb}$ ($x = 0.25, 0.5, 0.75, 1$) magnetic moment M_{tot}/N_{Mn} , Mn atom d-orbit magnetic moment M_{Mn} , Sb atom p-orbit magnetic moment M_{Sb} , ground state magnetic properties (GP) and Curie temperature T_C (K). Material properties (MPs) are also given.

x	M_{tot}/N_{Mn} (μ_B)	M_{Mn} (μ_B)	M_{Sb} (μ_B)	GP	T_C	MP
0.25	4	3.831	-0.075	FM	496	HMF
0.5	4	3.918	-0.124	FM	866	HMF
0.75	4	3.889	-0.156	FM	919	HMF
1	4 ⁴⁶	-	-	FM	587 ⁴⁷	HMF

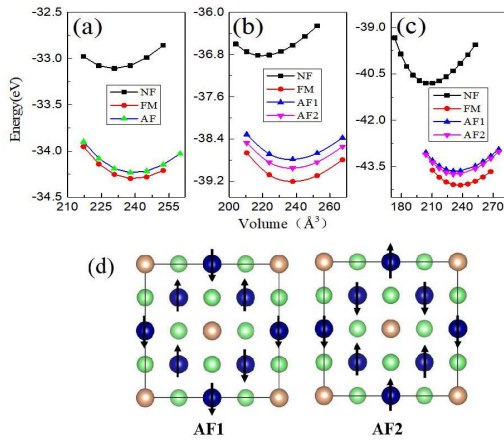


FIG. 2. Energy-volume curves of $\text{Ga}_{1-x}\text{Mn}_x\text{Sb}$ ($x = 0.25, 0.5, 0.75$) (a) $\text{Ga}_{0.75}\text{Mn}_{0.25}\text{Sb}$; (b) $\text{Ga}_{0.5}\text{Mn}_{0.5}\text{Sb}$; (c) $\text{Ga}_{0.25}\text{Mn}_{0.75}\text{Sb}$; (d) AF1 and AF2 stand for two different AFM states.

In their equilibrium lattice constants, the $\text{Ga}_{1-x}\text{Mn}_x\text{Sb}$ ($x = 0.25, 0.5, 0.75$) compounds have an integer magnetic moment (in a Bohr magneton, μ_B), corresponding to the FM HM nature. The average magnetic moment of a single Mn atom in $\text{Ga}_{1-x}\text{Mn}_x\text{Sb}$ ($x = 0.25, 0.5, 0.75$) is $4.0 \mu_B$. Fig.3 shows the total magnetic moment of these three FM HM materials, which varies with the lattice constant within 20%. The total magnetic moment remained constant for lattice changes between -5% and 25% . Additionally, we explored the magnetic moment contribution of each atom in the material. The total magnetic moment is dominated by the magnetic moment of the Mn- d orbital, and the contributions of other atomic magnetic

moments are small. Furthermore, the contributions of the Mn-*d* and Sb-*p* orbital magnetic moments are opposite each other. Fig.3 demonstrates that the magnetic moment changes of Mn-*d* increase with the increasing lattice constant, but this trend is gradual. Table I lists the magnetic moments and material properties of each atom. Next, we estimate the Curie temperature of the three FM half-metals using the mean field method⁴⁸⁻⁵⁰,

$$\frac{3}{2}k_B T = -\frac{\Delta E_{FM-AF}}{C} \quad (1)$$

where *C* represents the number of doped Mn atoms in the unit cell, and k_B represents the Boltzmann constant. All three compounds are found to have a Curie temperature above 400 K at room temperature. MnSb has been proven to be a FM half-metal with a Curie temperature of 587 K⁴⁷. Table I shows the magnetic properties and Curie temperature of Ga_{1-x}Mn_xSb ($x = 0.25, 0.5, 0.75, 1$).

Electronic properties. Fig.4 gives the energy band structures of Ga_{1-x}Mn_xSb ($x = 0.25, 0.5, 0.75$) compounds at their equilibrium lattice constants. The spin-up energy bands of Ga_{1-x}Mn_xSb ($x = 0.25, 0.5, 0.75$) straddle the Fermi level E_F , which is metallic, while the spin-down energy band has a gap, which indicates insulator behavior. Ga_{1-x}Mn_xSb has a conduction band bottom and a valence band top located at the high symmetry point Γ of the Brillouin zone, which is a direct band gap, and the band gap becomes wider as the Mn concentration increases, as shown in Table I. Therefore, the different characteristics exhibited by the spin-up and spin-down electron energy bands reveal that the ZB Ga_{1-x}Mn_xSb crystal has HM properties. We also used the same method to calculate the electronic structure of ZB GaSb and ZB MnSb by completely replacing Ga atoms, and we obtained the band diagram of the semiconductor GaSb with the direct band gap at the center of the Brillouin zone. MnSb is a FM half-metal, as shown in Fig.4(d), which agree with previous results. These two crystalline materials have long been studied, and our results are consistent with the electronic structures reported in the previous literature^{37,46}. By comparison, we found that the FM HM properties of Ga_{1-x}Mn_xSb ($x = 0.25, 0.5, 0.75, 1$) are caused by Mn atoms.

Table II shows the equilibrium lattice constants and ground state properties calculated for Ga_{1-x}Mn_xSb ($x = 0, 0.25, 0.5, 0.75, 1$) and related values from the literature. We determined that the Ga-Sb bond is 2.638 Å long when the semiconductor GaSb is for the equilibrium lattice constant. By comparing the bond lengths among the atoms in the series of FM

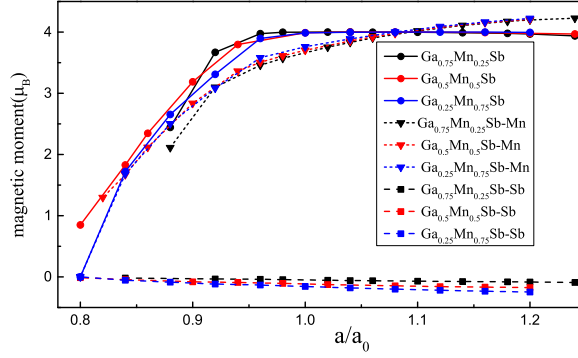


FIG. 3. Total magnetic moment and the contribution of the magnetic moment from the Mn- d and Sb- p orbitals as a function of the relative change in the lattice constant.

$\text{Ga}_{1-x}\text{Mn}_x\text{Sb}$ ($x = 0.25, 0.5, 0.75, 1$) shown in Table II, we can see that after doping with Mn, the outermost orbital electrons of Mn in $\text{Ga}_{1-x}\text{Mn}_x\text{Sb}$ ($x = 0.25, 0.5, 0.75, 1$) are consumed by the bond owing to the difference in electronegativity and the electron orbital interatomic hybridization. Because a larger Ga atom is substituted with a smaller Mn atom, the Mn-Sb bonds in the ZB structure are shorter than the Ga-Sb bonds. Table II demonstrates that the semiconductor band gap and the HM gap of HMF $\text{Ga}_{1-x}\text{Mn}_x\text{Sb}$ ($x = 0.25, 0.5, 0.75, 1$) both increase with increasing concentration. The minimum of the HM gap of a HM material is intermediate along the distance from the Fermi energy to either the valence band or the bottom of conduction band in the spin sub-band with a band gap⁵¹.

To further study the principle underlying the HM properties of this series of HMF materials, the total density of states of $\text{Ga}_{0.75}\text{Mn}_{0.25}\text{Sb}$ is selected because the electronic densities of the $\text{Ga}_{1-x}\text{Mn}_x\text{Sb}$ ($x = 0.25, 0.5, 0.75$) compounds are similar. Additionally, the atomic wave partial density of states is taken as an example. As Fig. 5 shows, the total electronic density of $\text{Ga}_{0.75}\text{Mn}_{0.25}\text{Sb}$ is metallic in the spin state near the Fermi surface, while the lower spin state has a clear band gap, indicating semiconductivity. Since only one spin-oriented electron exists at the Fermi level of $\text{Ga}_{0.75}\text{Mn}_{0.25}\text{Sb}$, the spin polarizability is defined as^{14,15}.

$$P = \frac{N_{\uparrow}(E) - N_{\downarrow}(E)}{N_{\uparrow}(E) + N_{\downarrow}(E)} \quad (2)$$

where N_{\uparrow} and N_{\downarrow} are the spin-up and spin-down density of states, respectively. We can conclude that the spin polarization of the conduction electrons of $\text{Ga}_{0.75}\text{Mn}_{0.25}\text{Sb}$ is 100%.

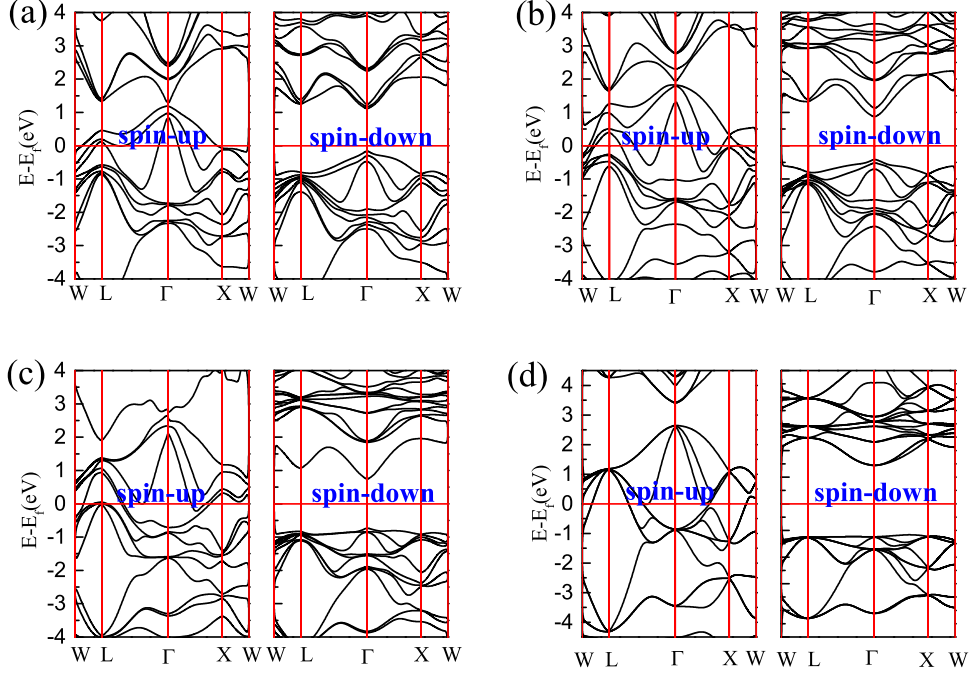


FIG. 4. Spin-dependent band structures of (a) $\text{Ga}_{0.75}\text{Mn}_{0.25}\text{Sb}$; (b) $\text{Ga}_{0.75}\text{Mn}_{0.25}\text{Sb}$; (c) $\text{Ga}_{0.25}\text{Mn}_{0.75}\text{Sb}$; (d) MnSb .

Because the electromagnetic and optical properties of most materials are derived from the intermetallic orbital pd , dd , and spd electron orbital hybridization, these properties are related to the electronic configuration of each atom and the electron orbital hybridization between atoms^{52–55}. Because the valence electronic configuration of Mn is $3d^54s^2$, and the valence electron configuration of Ga is $4s^24p^1$, the outermost $4p$ orbit has only one electron in Ga. Additionally, the valence electron configuration of Sb is $5s^25p^3$, and its $5p$ state has three electrons, which is the half-filled state (p -state full-shell layer is six electrons). Furthermore, comparing the bond length and density of states between individual atoms in the crystal suggests that strong hybridization occurs near the Fermi level. As Table II shows, the Mn-Sb bond length are shorter than that of the the Ga-Sb, indicating that the electron hybridization occurs mainly between the transition metal atom Mn and the Sb atom. The $3d$ orbital of Mn and the $5p$ orbital of Sb are found to undergo pd electron hybridization; therefore, the $3d$ electronic density distribution of Mn exhibits a shift in the energy level. In other words, electron orbital hybridization causes the total electronic density of crystal materials to redistribute, which is the main reason $\text{Ga}_{1-x}\text{Mn}_x\text{Sb}$ ($x = 0.25, 0.5, 0.75$) exhibits

FM HM properties.

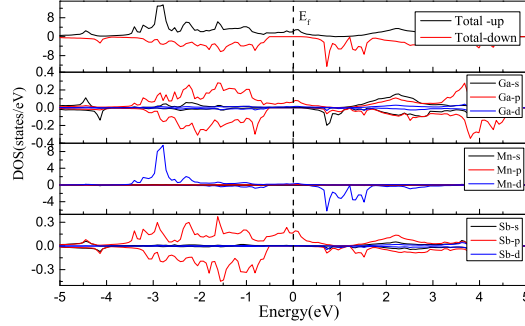


FIG. 5. Total electron density states and projected density states of $\text{Ga}_{0.75}\text{Mn}_{0.25}\text{Sb}$.

Optical Properties. The optical properties of a solid can be described by a dielectric function^{56,57}, which consists of a real part and an imaginary part and is defined as

$$\varepsilon(\omega) = \varepsilon_1(\omega) + i\varepsilon_2(\omega) \quad (3)$$

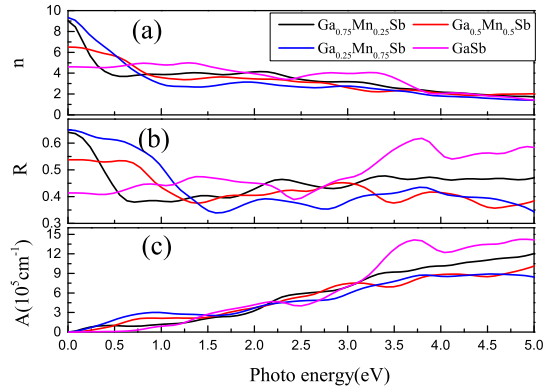


FIG. 6. Comparison of the calculated optical properties of $\text{Ga}_{1-x}\text{Mn}_x\text{Sb}$ ($x = 0, 0.25, 0.5, 0.75$): (a) optical refractive index; (a) optical reflectivity; (c) optical absorption coefficient.

Because $\text{Ga}_{1-x}\text{Mn}_x\text{Sb}$ ($x = 0.25, 0.5, 0.75$) belongs to the cubic system, its optical properties are known to be isotropic. In this study, the dielectric constant of $\text{Ga}_{1-x}\text{Mn}_x\text{Sb}$ ($x = 0.25, 0.5, 0.75$) is calculated, and the optical properties are analyzed. Fig.6 shows the relationship between the optical properties and the incident light energy, comparing the refractive index n , reflectance R , and absorption coefficient A of some crystalline materials.

We can use the real and imaginary parts of the dielectric function to obtain the absorption coefficient and reflectivity of the solid using the following formulas:

$$\alpha(\omega) = \sqrt{2}\omega\sqrt{\sqrt{\varepsilon_1^2(\omega) + \varepsilon_2^2(\omega)} - \varepsilon_1(\omega)} \quad (4)$$

$$R(\omega) = \left| \frac{\sqrt{\varepsilon(\omega)} - 1}{\sqrt{\varepsilon(\omega)} + 1} \right|^2 \quad (5)$$

TABLE II. Crystal properties of $\text{Ga}_{1-x}\text{Mn}_x\text{Sb}$, the equilibrium lattics constant a_0 (\AA), Mn-Sb bond length L_{MS} (\AA), Ga-Sb bond length L_{GS} (\AA), the HM gaps calculated by HSE and PBE, E_{HM-HSE} (eV) and E_{HM-PBE} (eV), respectively, the semiconductor gaps calculated by HSE and PBE, E_{HSE} (eV) and E_{PBE} (eV), respectively.

x	a_0	L_{MS}	L_{GS}	E_{HM-HSE}	E_{HM-PBE}	E_{HSE}	E_{PBE}
0	6.095	-	2.554	-	-	0.526	0.083
						0.720 ⁵⁸	0.110 ⁵⁸
0.25	6.208	2.663	2.697	0.144	0.086	1.239	0.593
0.5	6.315	2.678	2.689	0.405	-	1.260	0.452
0.75	6.179	2.671	2.696	0.723	-	1.455	0.746
1	6.178	2.675	-	0.988	-	2.217	1.457
	6.166 ⁵⁹				0.200 ⁵⁹		1.491 ⁵⁹
	6.166 ⁶⁰				0.150 ⁶⁰		0.900 ⁶⁰

Fig6(a) and 6(b) reveal that the static refractive index $n(0)=9$ of $\text{Ga}_{0.75}\text{Mn}_{0.25}\text{Sb}$ and the static reflectance are $R(0)=0.64$, respectively, which are higher than those of GaSb, i.e., $n(0)=4.6$ and $R(0)=0.41$, respectively. The calculation results revealed that the static refractive index and static reflectivity of Mn-doped FM materials are higher than those of GaSb. The refraction spectrum of $\text{Ga}_{1-x}\text{Mn}_x\text{Sb}$ ($x = 0.25, 0.5, 0.75$) in Fig. 6(a) demonstrates that in the energy range of $0 - 3.5$ eV, the refractive indices of these materials tend to decrease gradually with the increasing incident light energy, whereas they decrease rapidly in the energy range of visible light at $1.3 - 3.5$ eV. Furthermore, the refractive power of the material

for infrared light is much higher than that for ultraviolet light, and the static refractive index and the static reflectivity of the doped material are both higher than those of undoped GaSb. The reflection and refraction patterns of different Mn concentrations demonstrate that the variations in the refractive index and reflectivity are similar when doping is not higher than 50%, and the higher the doping concentration is, the more obviously the refractive index changes. Fig.6(c) reveals that in the energy range of 0 – 5 eV, the absorption coefficients of the four $\text{Ga}_{1-x}\text{Mn}_x\text{Sb}$ compounds tend to increase gradually. In the visible region, there is no obvious absorption peak, and the absorption coefficient of the material does not change much after doping with Mn. In contrast, in the infrared region, that is, when the incident photon energy below 1.3 eV, the effects of doping are obvious. The doped material absorbs significantly more infrared light than GaSb. Therefore, $\text{Ga}_{1-x}\text{Mn}_x\text{Sb}$ ($x = 0.25, 0.5, 0.75$) has a strong absorption capacity for infrared light and is suitable for use in electronic devices related to infrared detection.

This paper presents the electronic structure and the magnetic and optical properties of Mn-doped semiconductor GaSb studied using a first-principles calculation method. The spin-polarized electronic density of states of $\text{Ga}_{1-x}\text{Mn}_x\text{Sb}$ ($x = 0.25, 0.5, 0.75$) is calculated, and the electron band structure and magnetic moment show that $\text{Ga}_{1-x}\text{Mn}_x\text{Sb}$ ($x = 0.25, 0.5, 0.75$) shows HM ferromagnetism, electron spin polarization of 100% with an integer magnetic moment, a wide energy gap, and a HM gap. Additionally, the high Curie temperature indicates that HM $\text{Ga}_{1-x}\text{Mn}_x\text{Sb}$ can be widely used in spintronic devices. Furthermore, optical properties such as the reflection and refraction of this series of materials were studied, and the optical properties of the HM materials $\text{Ga}_{1-x}\text{Mn}_x\text{Sb}$ are found to be similar, with a large static reflection and static refractive index. In the visible light range, the absorption coefficient is small, but the infrared light absorption is strong. Therefore, the FM HM $\text{Ga}_{1-x}\text{Mn}_x\text{Sb}$ series is also a potential material for infrared photoelectric devices.

ACKNOWLEDGMENTS

This work was supported by the NSFC (Grants No.11874273), the Specialized Research Fund for the Doctoral Program of Higher Education of China (Grant No.2018M631760), the Project of Hebei Educational Department, China (No. ZD2018015 and QN2018012), the Advanced Postdoctoral Programs of Hebei Province (No.B2017003004) and the Key

Project of Sichuan Science and Technology Program (19YFSY0044). The numerical calculations in this paper have been done on the supercomputing system in the High Performance Computing Center of Yanshan University.

REFERENCES

- ¹G. A. Prinz, [Science](#) **282**, 1660–1663 (1998).
- ²H. Ohno, H. Munekata, T. Penney, S. Von Molnar, and L. Chang, [Physical Review Letters](#) **68**, 2664–2667 (1992).
- ³R. De Groot, F. Mueller, P. Van Engen, and K. Buschow, [Physical Review Letters](#) **50**, 2024–2027 (1983).
- ⁴S. Chen and Z. Ren, [Materials Today](#) **16**, 387–395 (2013).
- ⁵S. M. Watts, S. Wirth, S. Von Molnar, A. Barry, and J. Coey, [Physical Review B](#) **61**, 9621–9628 (2000).
- ⁶W.-H. Xie and B.-G. Liu, [Journal of Applied Pphysics](#) **96**, 3559–3561 (2004).
- ⁷B. Doumi, A. Mokaddem, L. Temimi, N. Beldjoudi, M. Elkeurti, F. Dahmane, A. Sayede, A. Tadjer, and M. Ishak-Boushaki, [The European Physical Journal B](#) **88**, 93–101 (2015).
- ⁸S. Wolf, D. Awschalom, R. Buhrman, J. Daughton, S. Von Molnar, M. Roukes, A. Y. Chtchelkanova, and D. Treger, [Science](#) **294**, 1488–1495 (2001).
- ⁹W. E. Pickett and J. S. Moodera, [Physics Today](#) **54**, 39–44 (2001).
- ¹⁰I. S. Osborne, [Science](#) **294**, 1483–1483 (2001).
- ¹¹D. D. Awschalom and J. M. Kikkawa, [Physics Today](#) **52**, 33–38 (1999).
- ¹²I. Žutić, J. Fabian, and S. D. Sarma, [Reviews of Modern Physics](#) **76**, 323–410 (2004).
- ¹³M. Katsnelson, V. Y. Irkhin, L. Chioncel, A. Lichtenstein, and R. A. de Groot, [Reviews of Modern Physics](#) **80**, 315–378 (2008).
- ¹⁴S. Chadov, T. Graf, K. Chadova, X. Dai, F. Casper, G. H. Fecher, and C. Felser, [Physical Review Letters](#) **107**, 047202 (2011).
- ¹⁵V. Alijani, J. Winterlik, G. H. Fecher, S. S. Naghavi, and C. Felser, [Physical Review B](#) **83**, 1–7 (2011).
- ¹⁶J. Coey, [Solid State Sciences](#) **7**, 660–667 (2005).
- ¹⁷K. Yang, R. Wu, L. Shen, Y. P. Feng, Y. Dai, and B. Huang, [Physical Review B](#) **81**, 125211–125215 (2010).

- ¹⁸H. Katayama-Yoshida and K. Sato, *Physica B: Condensed Matter* **327**, 337–343 (2003).
- ¹⁹M. Hass and B. Henvis, *Journal of Physics and Chemistry of Solids* **23**, 1099–1104 (1962).
- ²⁰H. Ehrenreich, *Journal of Applied Physics* **32**, 2155–2166 (1961).
- ²¹Y. Liu and B. G. Liu, *Journal of Physics D: Applied Physics* **40**, 6791–6796 (2007).
- ²²N. Noor, S. Ali, and A. Shaukat, *Journal of Physics and Chemistry of Solids* **72**, 836–841 (2011).
- ²³G. Rahman, S. Cho, and S. C. Hong, *Physica Status Solidi* **244**, 4435–4438 (2010).
- ²⁴M. Shirai, *Physica E: Low-dimensional Systems and Nanostructures* **10**, 143–147 (2001).
- ²⁵A. Milnes and A. Polyakov, *Solid State Electronics* **36**, 803–818 (1993).
- ²⁶H. I. Zhang and J. Callaway, *Physical Review* **181**, 1163–1172 (1969).
- ²⁷R. Ahmed, S. J. Hashemifar, H. Rashid, H. Akbarzadeh, *et al.*, *Communications in Theoretical Physics* **52**, 527–533 (2009).
- ²⁸W. F. Schottky and M. B. Bever, *Acta Metallurgica* **6**, 320–326 (1958).
- ²⁹B. Bennett and R. Soref, *IEEE journal of quantum electronics* **23**, 2159–2166 (1987).
- ³⁰D. E. Aspnes and A. Studna, *Physical Review B* **27**, 985–1009 (1983).
- ³¹Y. Wei, A. Gin, M. Razeghi, and G. J. Brown, *Applied Physics Letters* **81**, 3675–3677 (2002).
- ³²M. Kondrin, S. Popova, V. Gizatullin, O. Sazanova, N. Kalyaeva, A. Lyapin, V. Brazhkin, A. Pronin, S. Gudoshnikov, and Y. V. Prokhorova, *Journal of Physics: Conference Series* **121**, 032011 (2008).
- ³³N. Seña, A. Dussan, F. Mesa, E. Castaño, and R. González-Hernández, *Journal of Applied Physics* **120**, 051704 (2016).
- ³⁴I. Galanakis and P. Mavropoulos, *Physical Review B* **67**, 104417 (2003).
- ³⁵I. Ahmad and B. Amin, *Computational Materials Science* **68**, 55–60 (2013).
- ³⁶G. Dresselhaus, *Physical Review* **100**, 580–586 (1955).
- ³⁷M. L. Cohen and T. Bergstresser, *Physical Review* **141**, 789–796 (1966).
- ³⁸G. Kresse and J. Hafner, *Physical Review B* **48**, 13115–13118 (1993).
- ³⁹G. Kresse and J. Furthmüller, *Physical Review B* **54**, 11169–11186 (1996).
- ⁴⁰G. Kresse and D. Joubert, *Physical Review B* **59**, 1758–1775 (1999).
- ⁴¹J. P. Perdew, J. A. Chevary, S. H. Vosko, K. A. Jackson, M. R. Pederson, D. J. Singh, and C. Fiolhais, *Physical Review B* **46**, 6671–6687 (1992).
- ⁴²J. P. Perdew, K. Burke, and M. Ernzerhof, *Physical Review Letters* **77**, 3865–3868 (1996).
- ⁴³E. R. Batista, J. Heyd, R. G. Hennig, B. P. Uberuaga, R. L. Martin, G. E. Scuseria,

- C. Umrigar, and J. W. Wilkins, *Physical Review B* **74**, 121102 (2006).
- ⁴⁴J. Heyd, G. E. Scuseria, and M. Ernzerhof, *The Journal of Chemical Physics* **118**, 8207–8215 (2003).
- ⁴⁵W. Kohn and L. J. Sham, *Physical Review* **140**, A1133–A1138 (1965).
- ⁴⁶J. C. Zheng and J. W. Davenport, *Physical Review B* **69**, 144415 (2004).
- ⁴⁷S. Popova, O. Sazanova, V. Brazhkin, N. Kalyaeva, M. Kondrin, and A. Lyapin, *Physics of the Solid State* **48**, 2177–2182 (2006).
- ⁴⁸Y. C. Cheng, Z. Y. Zhu, W. B. Mi, Z. B. Guo, and U. Schwingenschlgl, *Physical Review B* **87**, 1214–1222 (2013).
- ⁴⁹T. Fukushima, K. Sato, H. Katayama-Yoshida, and P. Dederichs, *Japanese Journal of Applied Physics* **43**, L1416–L1418 (2004).
- ⁵⁰E. Şaşıoğlu, L. Sandratskii, and P. Bruno, *Physical Review B* **70**, 024427 (2004).
- ⁵¹F. Zheng, G. Zhou, Z. Liu, J. Wu, W. Duan, B.-L. Gu, and S. Zhang, *Physical Review B* **78**, 205415 (2008).
- ⁵²R. De Paiva, R. Nogueira, and J. Alves, *Journal of Applied Physics* **96**, 6565–6568 (2004).
- ⁵³Z.-Y. Chen, B. Xu, and G. Gao, *Journal of Magnetism and Magnetic Materials* **347**, 14–17 (2013).
- ⁵⁴S. Arif, I. Ahmad, and B. Amin, *International Journal of Quantum Chemistry* **112**, 882–888 (2012).
- ⁵⁵A. Nabi, Z. Akhtar, T. Iqbal, A. Ali, and M. A. Javid, *Journal of Semiconductors* **38**, 073001 (2017).
- ⁵⁶J. P. Perdew, K. Burke, and M. Ernzerhof, *Physical Review Letters* **77**, 3865–3868 (1996).
- ⁵⁷G. Kresse and J. Furthmüller, *Physical Review B* **54**, 11169–11186 (1996).
- ⁵⁸Y.-S. Kim, M. Marsman, G. Kresse, F. Tran, and P. Blaha, *Physical Review B* **82**, 205212 (2010).
- ⁵⁹S.-D. Guo and B.-G. Liu, *Europhysics Letters* **93**, 47006 (2011).
- ⁶⁰L.-J. Shi and B.-G. Liu, *Journal of Physics: Condensed Matter* **17**, 1209–1216 (2005).